communications earth & environment

Article

A Nature Portfolio journal

https://doi.org/10.1038/s43247-025-02585-7

# Global South shows higher urban flood exposures than the Global North under current and future scenarios

Check for updates

**Qian Zhang[1,2], Chunlin Li[1,3,4] ✉, Ding Wen[5] ✉, Jieming Kang[1,2], Tan Chen[6], Baolei Zhang[2], Yuanman Hu[1,3], Jiabo Yin[7] & Louise Slater[8]**

Urbanization has intensified in recent decades, raising concerns about increasing flood exposure in cities. Here, we assess urban flood exposure in terms of built-up area, population, and economic activity located within zones affected by 1-in-100-year river flood events. We use global historical data from 2000 to 2020 and future projections from 2030 to 2100 under the Shared Socioeconomic Pathways. From 2000 to 2020, global urban flood exposure increased substantially, with the most severe impacts in East Asia and the fastest growth in Africa. Future exposure continues to rise, especially under high-risk development scenarios. From 2030 to 2100, flood-exposed urban area, population, and economy in Global South are more than twice, nearly five times, and over twice those in Global North, respectively. Inequality in exposure is greater within developing regions than developed ones. These disparities are projected to widen, highlighting the urgent need for targeted, region-specific strategies to reduce flood risks.

With the intensification of global climate change, the frequency and intensity of extreme weather are continuously increasing, particularly heavy rainfall, which can trigger excessive runoff and considerably raise the likelihood of flooding[1]. Meantime, the rapid urbanization process has further exacerbated urban flood risks, posing serious threats to buildings, residents, infrastructures, and properties within cities[2]. On one hand, large areas of natural land have been converted into impervious surface (e.g., concrete and asphalt), hindering natural water infiltration and leading to a substantial increase in surface runoff, making cities more vulnerable to floods during heavy rainfall events[3,4]. On the other hand, the urbanization process is often accompanied by a high concentration of population and property, which exacerbates the severity of losses when floods occur[5]. Currently, ~57% of the global population resides in urban areas, and is expected to rise to 68% by 2050[6,7]. Furthermore, future socioeconomic changes are highly concerned to further intensify urban flood disasters[8,9]. Therefore, understanding the historical evolution and future trends of urban flood exposures is crucial for achieving sustainable urban development.

Over the past decades, urban floods have caused tens of billions of dollars in property damage and substantial loss of life. Scholars have studied flood exposure issues from various scales, including global[10], national[11], subnational[12], urban agglomerations[13], river delta[1], and individual cities[14]. Researches indicate a marked increase in urban flood exposures, with East Asia (particularly China) facing the highest risks. The distribution of urban flood exposures across regions exhibits pronounced heterogeneity[15]. Low-income and underdeveloped countries often lack sufficient resources to cope with flood disasters, making urban flood exposures more severe in these regions[16]. Currently, ~1.81 billion people globally are facing a 1-in-100-year flood risk, with 89% residing in low- and middle-income countries[12]. The impacts of floods are particularly severe in these countries, causing not only direct loss of life and property damage but also far-reaching effects on long-term economic development, social stability, and public health[17,18]. Previous studies have investigated the impact of income and demographics on urban flood exposure inequality, finding that low-income and Black populations often live in flood-prone areas lacking flood defenses and adequate emergency response measures, thus facing higher urban flood exposures[19,20]. These unequal exposures suggest that global strategies and resource allocation for addressing flood disasters need to focus more on vulnerable areas to reduce regional inequalities and enhance global

[1]CAS Key Laboratory of Forest Ecology and Silviculture, Institute of Applied Ecology, Chinese Academy of Sciences, Shenyang, China. [2]College of Geography and Environment, Shandong Normal University, Jinan, China. [3]E'erguna Wetland Ecosystem Research Station, Hulunbuir, China. [4]Liaoning Shenyang Urban Ecosystem Observation and Research Station, Shenyang, China. [5]South China Institute of Environmental Science, Ministry of Ecology and Environment, Guangzhou, China. [6]State Key Laboratory of Lake and Watershed Science for Water Security, Nanjing Institute of Geography and Limnology, Chinese Academy of Sciences, Nanjing, China. [7]State Key Laboratory of Water Resources Engineering and Management, Wuhan University, Wuhan, China. [8]School of Geography and the Environment, University of Oxford, Oxford, UK. ✉e-mail: lichunlin@iae.ac.cn; wending@scies.org

disaster response capacity. Therefore, assessing the spatiotemporal patterns of urban flood exposures, identifying high-exposure areas, and revealing their inequality are crucial for developing more targeted and sustainable urban planning strategies.

With socioeconomic development and the increasing frequency of urban flooding driven by climate change, urban flood exposures are expected to rise in the future[21]. Direct economic losses[22], indirect economic losses[2], urban areas exposed to floods[23], and population exposure[24] were used as indicators of urban flood exposures to explore trends under different future scenarios, and indicated that under high-emission and high-warming scenarios, urban flood exposures will substantially increase[1,16]. The Global South often faces challenges such as poverty, inadequate infrastructure, and resource shortages[25], making it more vulnerable to urban flood exposures and even exacerbating its losses from such disasters in future scenarios[5].

While existing studies have explored global flood exposure from various perspectives, such as historical dynamics of flood-prone urban areas[10], future population-driven exposure projections[26], and inequality in flood risks[5], several critical gaps remain. First, most previous research has focused on a single exposure dimension (e.g., urban area or population), lacking a comprehensive, multi-dimensional assessment. Second, the role of urban expansion in shaping future flood exposure has not been sufficiently investigated. Third, while some studies have examined inequality in flood risk, few have analyzed how such disparities evolve over time under different future socioeconomic scenarios.

To fill these gaps, we analyze urban flood exposure across historical (2000–2020) and future periods (2030–2100) under various Shared Socioeconomic Pathways (SSPs), covering multiple spatial scales, including global, national, subnational, and the Global South–North divide. Specifically, our objectives are: (1) Identifying the historical evolution of urban flood exposures from 2000 to 2020 and outlining its trends at global and regional scales, (2) Analyzing the trends and spatial distribution of flood exposures in newly built-up areas, (3) Evaluating the future urban flood exposures under different SSPs from 2030 to 2100, (4) Revealing the inequality of urban flood exposures between Global South and Global North. Focusing specifically on river flooding, one of the most frequent and destructive flood types globally, our findings contribute to a better understanding of the interactions among urbanization, socioeconomic development, and flood risk. The results provide valuable insights for climate adaptation, disaster risk reduction, and equitable urban planning strategies.

## Results

### Historical urban flood exposures

From 2000 to 2020, urban areas exposure to urban flooding (UEF), population exposure to urban flooding (PEF), and economic exposure to urban flooding (EEF) have shown considerable global increases, with respective growth rates of 254.66%, 135.05%, and 181.09%, indicating an overall rise in urban flood exposures (Fig. 1). Among subcontinental regions, East Asia stands out for its remarkable increase, with UEF growing from $1.82 \times 10^{10}$ km$^2$ to $9.62 \times 10^{10}$ km$^2$, PEF rising from $9.31 \times 10^7$ to $2.28 \times 10^8$, and EEF expanding from $1.58 \times 10^{12}$ USD to $6.48 \times 10^{12}$ USD, particularly between 2015 and 2020. These results highlight the escalating urban flood exposures driven by rapid urbanization and the concentration of population and assets. Other regions, such as North America, Southeast Asia, and South Asia, also exhibit high values for UEF, PEF, and EEF, emphasizing their prominent roles in global urban flood exposures. However, the average annual growth rate (AAGR) varies considerably (Supplementary Table S1). For example, North America, despite its relatively high UEF, had the lowest AAGR at 2.92%. In contrast, East Africa and Central Asia, while having relatively low UEF, recorded the highest AAGR—14.37% and 12.67%, respectively. This trend is also reflected in PEF and EEF, suggesting that these regions are undergoing rapid urbanization and becoming increasingly vulnerable to urban flooding.

While most regions experienced increasing trends in UEF and PEF from 2015 to 2020, several economically developed areas showed a decline in EEF. This pattern is particularly evident in North America, Central America, Southern Europe, and Northern Europe. A summary of key regions with notable decreases in EEF and PEEF is provided in Supplementary Table S2. For instance, New York (−9.13 billion USD), Lazio (−17.43 billion USD), and England (−18.65 billion USD) all experienced notable reductions in EEF, both in absolute terms and relative to their regional GDP (PEEF). Interestingly, in some of these regions, such as New Jersey, although the exposed urban area and population increased, their proportional exposure (PUEF and PPEF) declined, suggesting that new development may have shifted to lower-risk zones. These trends likely reflect the influence of land-use regulation, economic restructuring, and strategic investment in protective infrastructure. However, it is important to note that despite these localized declines, most regions in North America, Central America, Southern Europe, and Northern Europe still experienced increases in UEF and PEF, indicating that the overall trend across these subcontinents remains one of rising flood exposure, albeit with important regional differences. These findings highlight a nuanced picture: although most regions within North America, Central America, Southern Europe, and Northern Europe experienced rising trends in UEF and PEF, there are exceptions where economic exposure decreased due to effective spatial planning and resilience investments. Such cases illustrate how policy and planning can offset some of the risks associated with urban expansion, even if the overall exposure continues to rise.

At the subnational scale in 2020, UEF, PEF, and EEF exhibit pronounced spatial variations (Fig. 2). Urban flood exposures of UEF, PEF, and EEF are highest in eastern coastal cities in Asia, especially in China. Developed countries like the USA and Japan have the highest EEF, while developing countries such as China and India have the highest PEF and UEF. Furthermore, subnational regions in economically developed areas, such as Germany, France, and South Korea, also exhibit high levels of EEF. Several regions in Africa, Central America, and Southeast Asia, such as Suriname, Liberia, Guyana, and Chad, have relatively low UEF, PEF, and EEF values compared to major urban centers like China and the USA. However, their PUEF, PPEF, and PEEF are markedly higher (Fig. 3). From the spatial perspective, these high-exposure proportion regions are concentrated between 30°N and 30°S, particularly in low-latitude developing regions. For instance, Suriname and Guyana in northern South America, and Liberia in West Africa, show PUEF exceeding 50%, indicating that the majority of their urban areas are exposed to flooding. Similarly, despite having smaller total populations and economies, Iraq, Chad, and Cambodia exhibit high PPEF and PEEF values, indicating much higher exposure proportions to flooding and potentially greater losses during flooding.

### Urban flood exposures in newly built-up areas

From 2000 to 2020, UEF, PEF, and EEF in newly built-up areas globally showed substantial increases, with UEF rising by $7.41 \times 10^{10}$ km$^2$, PEF increasing by $2.17 \times 10^8$, and EEF growing by $2.15 \times 10^{12}$ USD (Fig. 4). The most notable growth occurred between 2015 and 2020, with UEF, PEF, and EEF increasing by 285.69%, 207.96%, and 169.83%, respectively, compared to the previous period. These trends reflect that, as urbanization accelerates, flood-prone zones are increasingly being converted into urban land, highlighting the direct impact of rapid urban growth on urban flood exposures. However, it is worth noting that the proportions of population and economic activity exposed to flooding within newly built-up areas (i.e., PPEF and PEEF) have decreased or remained stable in many regions from 2000 to 2020. This is because our analysis specifically focuses on newly built-up urban areas, where PPEF and PEEF represent the shares of newly added urban population and economic activity located in flood-prone zones. While the total urban land exposed to flooding (that is, UEF) has increased, the shares of population and economic activity exposed within newly developed urban areas have not shown a corresponding increase. This indicates that, in many cases, the proportion of new development occurring in flood-prone zones has remained relatively stable over time.

There are regional differences in urban flood exposures in newly built-up areas (Fig. 4). UEF, PEF, and EEF in newly built-up areas in East Asia increased markedly, accounting for over half (54.24%, 55.64% and 63.72%,

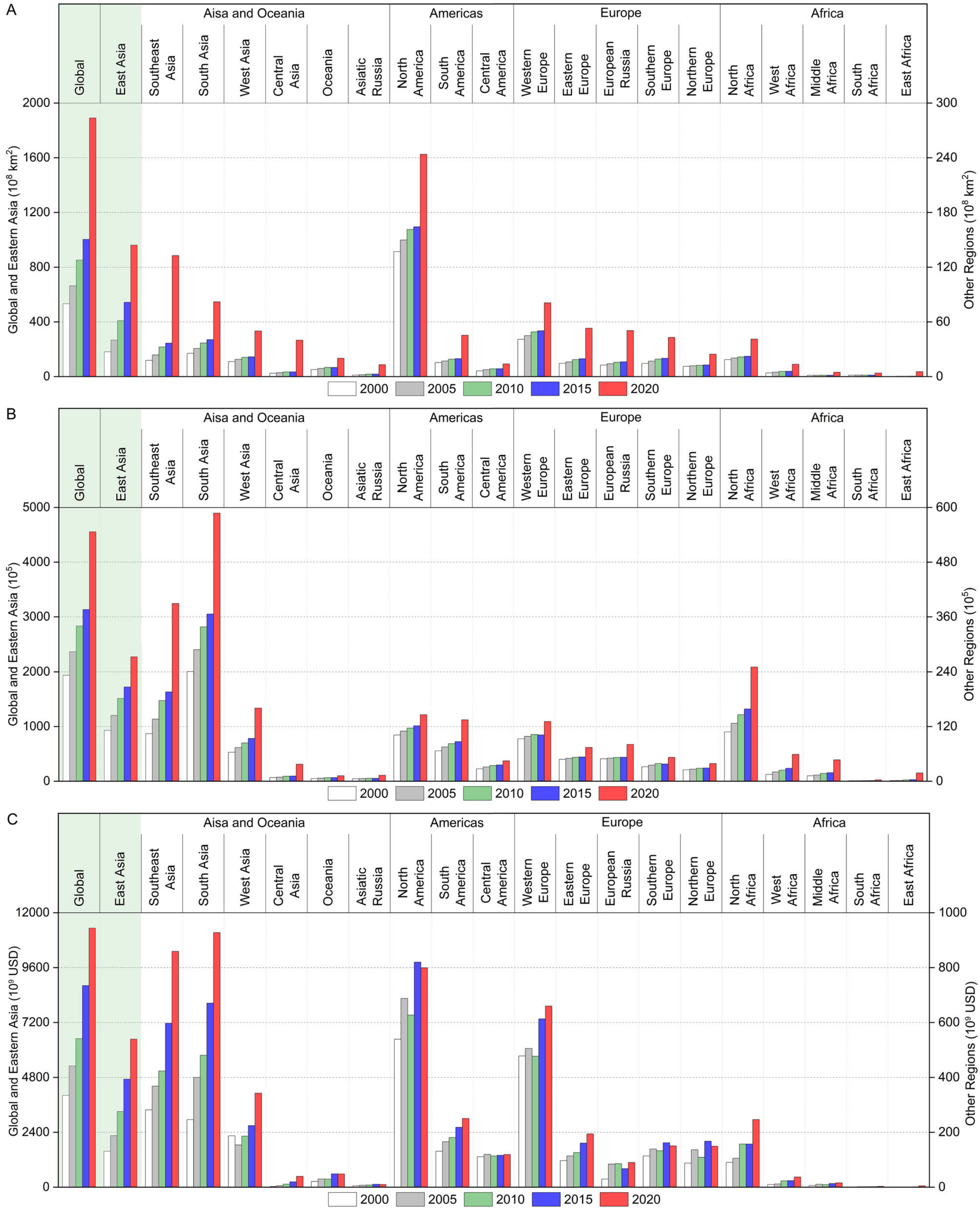


**Fig. 1 | Historical urban flood exposures at global and subcontinental scales.** Global and East Asia are on the left vertical axis, and the other regions are on the right vertical axis. The bar colors from left to right are white, gray, green, blue, and red, representing the years 2000, 2005, 2010, 2015, and 2020, respectively. **A** UEF; **B** PEF; **C** EEF.

respectively) of the global newly built-up areas in the flood-prone zone. PUEF in newly built-up areas in East Asia was 14.14% from 2000 to 2020, nearly 1.94 times the global average value (7.29%), indicating the region's disproportionately high urban flood exposures. North America and Europe displayed increases in PUEF, PPEF, and PEEF in newly built-up areas, especially between 2015 and 2020. However, PUEF, PPEF, and PEEF in these regions are relatively stable compared to the global average. South America also showed increases in UEF, PEF, and EEF in newly built-up

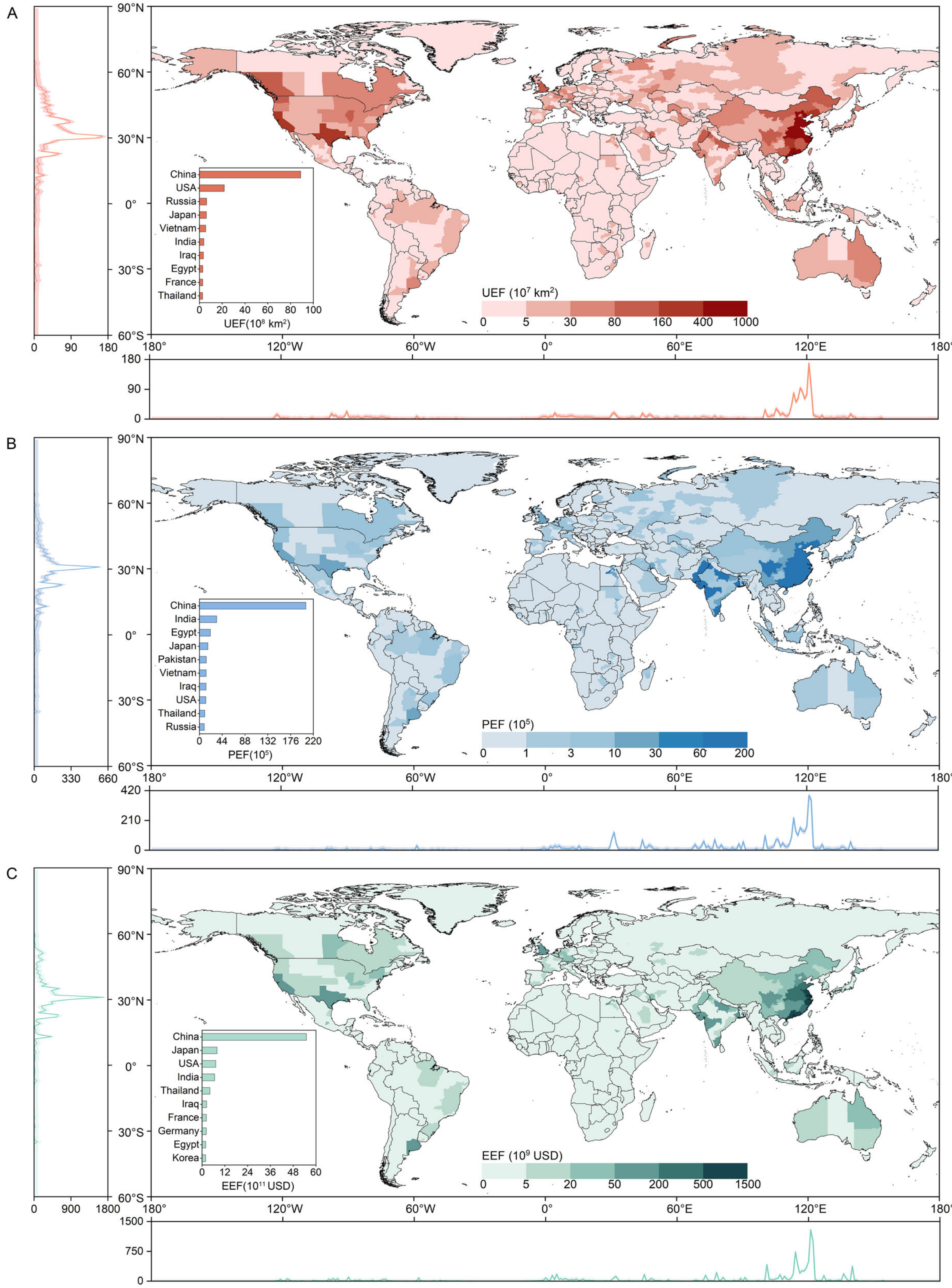


**Fig. 2 | Urban flood exposures at subnational scales in 2020 and the ten countries with the highest urban flood exposures.** The line charts on the left represent the variation of values along latitude, while the line charts at the bottom represent the variation of values along longitude. **A** UEF. **B** PEF. **C** EEF.

areas, which reflects rapid urbanization and growing vulnerability. North and West Africa indicated notable increases in PEF in newly built-up areas, indicating growing population vulnerability to floods. Middle, South, and East Africa, with slower urbanization rates, showed lower levels of UEF, PEF, and EEF in newly built-up areas, but they are still experiencing gradual increases due to urban expansion and growing populations.

The scattered distribution of circles in Fig. 5 indicated notable spatial variation of urban flood exposures in newly built-up areas across

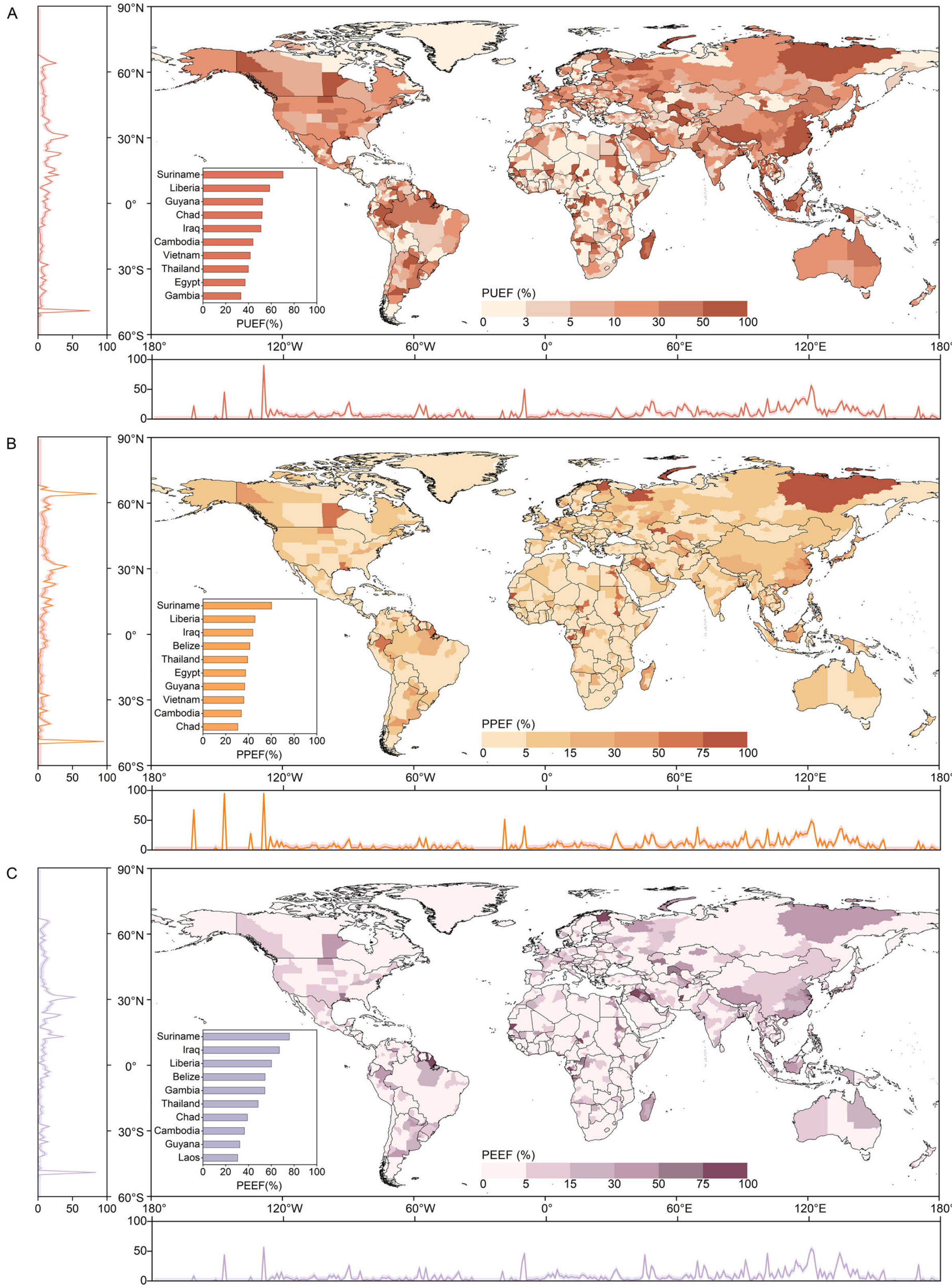


**Fig. 3 | Proportion of urban flood exposures at subnational scales in 2020 and the ten countries with the highest exposure proportion.** The line charts on the left represent the variation of values along latitude, while the line charts at the bottom represent the variation of values along longitude. **A** Proportion of urban areas exposure to urban flooding (PUEF); **B** Proportion of population exposure to urban flooding (PPEF); **C** Proportion of economic exposure to urban flooding (PEEF).

subnational regions globally from 2000 to 2020. Asian regions, predominantly located in the first quadrant, face higher urban flood exposures. These regions account for a larger share of urban expansion and have higher proportions of population and economic exposure, making them more susceptible to the devastating impacts of urban flooding. Some African regions (orange dots) exhibit particularly high economic exposure, while exposures related to urban areas and population are more dispersed. Europe (green dots) and South America (purple dots) show scattered urban flood

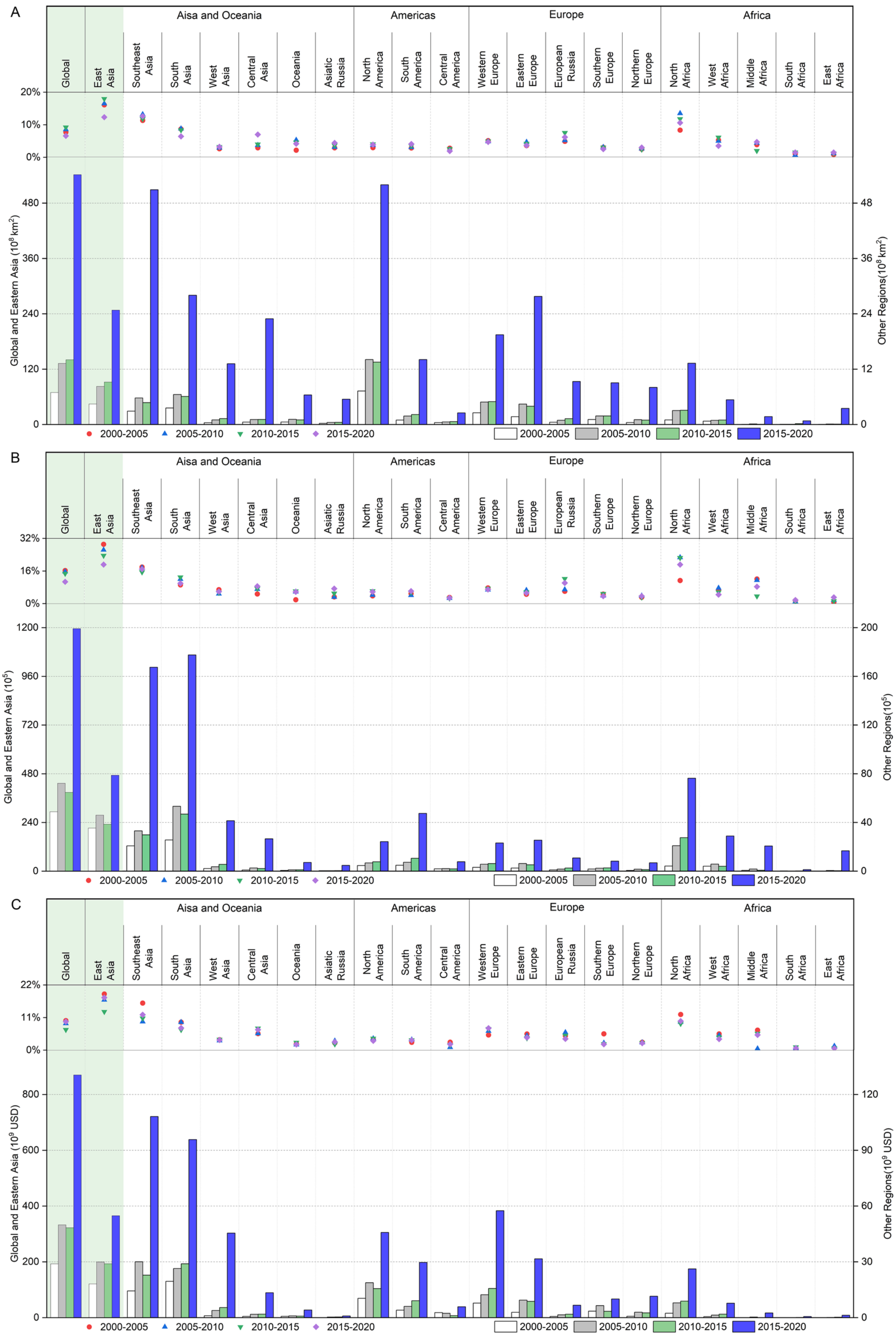


**Fig. 4 | Flood exposures in newly built-up urban areas from 2000 to 2020.** The scatter plots show the proportion of newly added urban land, population, and economic activity located in flood-prone areas. The shapes in the scatter plots represent different time intervals: circles for 2000–2005, upward triangles for 2005–2010, downward triangles for 2010–2015, and diamonds for 2015–2020. The bar charts show the absolute amount of newly developed urban land, population, and economy exposed to flooding. The bar colors from left to right are white, gray, green, and blue, corresponding respectively to 2000–2005, 2005–2010, 2010–2015, and 2015–2020. **A** UEF and PUEF. **B** PEF and PPEF. **C** EEF and PEEF.

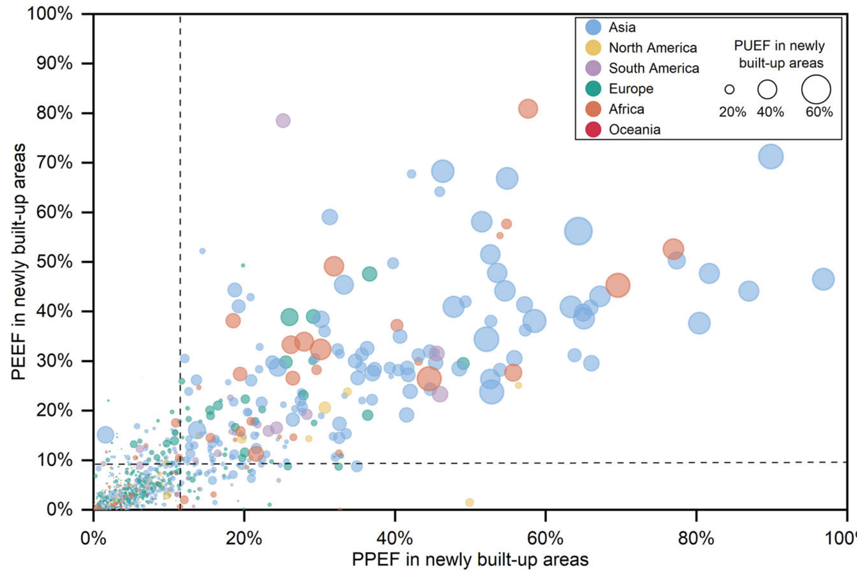


**Fig. 5 | Urban flood exposures in newly built-up areas at the subnational scale (2000–2020 average).** Circle size represents the PUEF in the total newly built-up area, and circle color indicates the continent: blue for Asia, yellow for North America, purple for South America, green for Europe, orange for Africa, and red for Oceania. The horizontal line marks the global average of PEEF, while the vertical line marks the global average of PPEF in newly built-up areas. The quadrants are labeled counter-clockwise from the top-right as the first, second, third, and fourth quadrants.

exposures, with relatively low proportions of economic and population exposure, mainly concentrated in the third quadrant. Newly built-up areas in North America (yellow dots) and Oceania (red dots) are generally less affected by urban flooding, although certain regions still exhibit notable economic and population exposure. Regions in the second quadrant and fourth quadrant show more mixed patterns, with high or low exposure in either population or economic terms, but relatively less pronounced overall exposure. These regions likely exhibit some urban expansion in the floodplain, but with lower population and economic concentration.

### Future urban flood exposures

The global UEF, PEF, and EEF were projected to continue rising, but the spatial distribution will largely remain consistent with historical patterns (Supplementary Fig. S1), with high values concentrated in East Asia, South Asia, and the western and southern regions of the United States. PUEF, PPEF, and PEEF exhibited more varied patterns, and the magnitude of their changes from 2030 to 2100 is detailed in Supplementary Fig. S2. Overall, PUEF and PPEF demonstrated a notable upward trend in most scenarios, whereas changes in PEEF showed large regional and scenario-specific variations, with declines observed in some regions and scenarios. Rapidly urbanizing and economically growing regions typically experienced substantial increases in PUEF, PPEF, and PEEF, particularly under SSP3 and SSP5 scenarios. In contrast, developed regions (e.g., Western and Northern Europe) exhibited a declining trend under SSPs, suggesting that rational planning and flood prevention measures were crucial for reducing urban flood exposures. Future efforts must prioritize high-exposure regions, such as Africa, South Asia, and Southeast Asia, to reduce inequalities in urban flood exposure by enhancing adaptive capacity and fostering regional cooperation.

Specifically, at the global scale, PUEF increased most markedly under SSP3 (5.84%) and decreased slightly under SSP1 (−1.34%), indicating that regional competition and unsustainable urbanization may lead to further development of flood-prone zones as built-up areas—a trend effectively mitigated by the sustainable development pathway of SSP1. At the regional level, regions such as Southeast Asia, South Asia, and Central Africa experienced notable increases in PUEF under all scenarios, particularly in Central Africa, where the growth rate reached 108.50% under SSP3. This may be closely linked to rapid urban expansion and lower flood resilience in these regions. PPEF increased markedly in almost all scenarios and regions, particularly under SSP3 and SSP5. For instance, Southeast Asia experienced a PPEF growth of 50.77% under SSP3, with growth exceeding 100% in Central Africa and East Africa. This suggests that the rapid concentration of urban populations in the future may expose more people to floods. However, some developed regions, such as Northern and Western Europe, exhibited a decrease in PPEF under SSP1 and SSP2, with Northern Europe showing a decline of 18.57% under SSP1. This implies that population exposures in these regions can be reduced through rational population distribution, which involves concentrating populations and infrastructure away from flood-prone areas, strengthening land-use planning, and promoting urban development in safer locations through effective policy measures, along with effective flood management.

### Inequality in urban flood exposures

Global urban flood exposures exhibit pronounced inequalities across time periods and different scenarios. From 2000 to 2020, the Gini coefficient of UEF, PEF, and EEF remained consistently high at 0.94–0.97, indicating a highly uneven global distribution of these metrics (Supplementary Table S3). The Gini coefficient of PUEF was relatively low, standing at 0.81 in 2020, indicating a relatively balanced distribution of urban flood-exposed areas. Meanwhile, the Gini coefficient of PPEF and PEEF decreased from 0.92 and 0.91 in 2000 to 0.84 and 0.85 in 2020, reflecting a gradual reduction in inequalities in flood-exposed population and economic proportions. Future projections under SSPs suggested that the Gini coefficient for these metrics will remain stable or slightly decline, but inequalities in global urban flood exposures were likely to persist at high levels. Spatially, a grid-based analysis of urban flood exposures was conducted, including hotspot and coldspot assessments. The results indicated that prominent flood hotspots (red dots) were concentrated in regions such as East Asia, South Asia, and North Africa, which are high-exposure zones for urban flood exposures (Fig. 6).

From the perspective of the Global South and Global North, urban flood exposures were markedly higher in the Global South compared to the Global North. In 2020, UEF, PEF, and EEF in the Global South were $1.30 \times 10^{11}$ km$^2$, $3.77 \times 10^8$, and $8.23 \times 10^{12}$ USD, respectively, which were 2.09, 4.77, and 2.57 times higher than those in the Global North. The PUEF, PPEF, and PEEF in the Global South were 2.51, 1.99, and 2.66 times higher than those in the Global North, respectively. These data clearly revealed the greater urban flood exposures in the Global South. Under various SSPs, the gap of urban flood exposures between the Global South and Global North (defined the exposure in the Global South minus that in the Global North) increased from 2030 to 2100, particularly for UEF and EEF (Fig. 6). Regarding UEF, the gap between the Global South and Global North remains stable under SSP1, markedly increased under SSP3, and decreased under SSP5. For PEF, the gap between the Global South and Global North

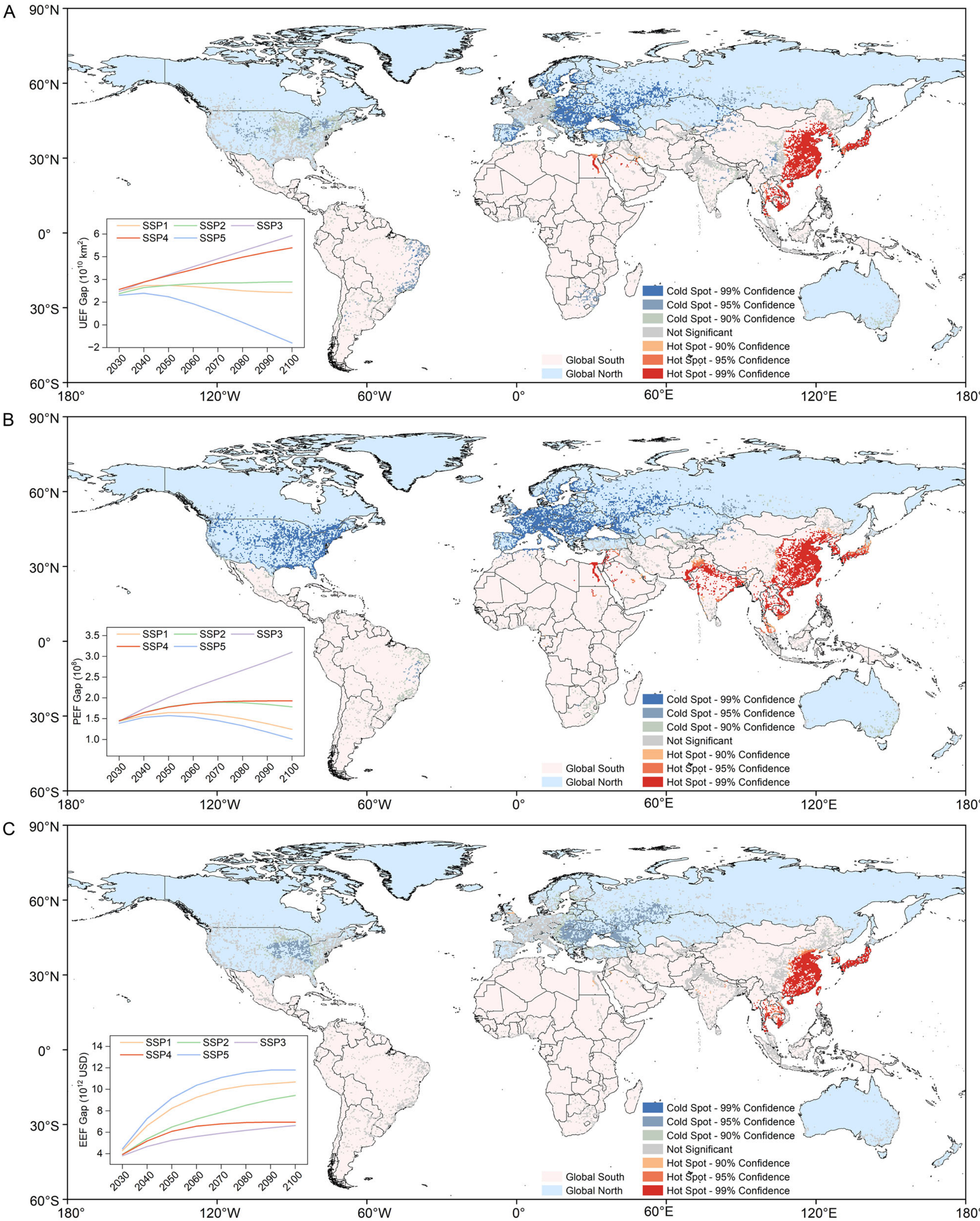


**Fig. 6 | Inequality in urban flood exposures.** The map shows the hotspots of global urban flood exposures in 2020, and the line graphs show the difference in urban flood exposures between the Global South and the Global North in the future from 2030 to 2100. In the map, the pink background indicates the Global South and the blue background indicates the Global North. In the hotspot analysis, red dots represent statistically significant hotspots, while blue dots represent coldspots. In the line graphs, orange represents SSP1, green represents SSP2, purple represents SSP3, red represents SSP4, and blue represents SSP5. **A** UEF. **B** PEF. **C** EEF.

increased across all scenarios, with the largest rise under SSP3. The EEF gap between the Global South and Global North increased most rapidly under SSP5, illustrating the substantial influences of economic development patterns on inequalities of urban flood exposures. These findings emphasized the considerable challenges of flood management in the Global South, requiring improvements in urban infrastructure resilience and long-term strategies to mitigate the impacts of global development patterns on regional flood exposures.

From 2000 to 2020, the Gini coefficient in the Global South consistently exceeded those in the Global North, with the ratios ranging from 1.04 to 1.17, indicating more pronounced inequality in the Global South (Supplementary Table S4). Meanwhile, the Gini coefficient ratios for UEF, PEF, and EEF increased from 1.06, 1.08, and 1.04 in 2000 to 1.10, 1.14, and 1.05 in 2020, indicating a continued deterioration in inequality regarding urban flood exposure distribution in the Global South. In 2030–2100, the Gini coefficient in the Global South remains consistently higher than that in the Global North, and the situation is expected to stay stable, reflecting the persistent difficulty in bridging the inequality gap between these regions.

## Discussion

Variations in socioeconomic and environmental factors lead to diverse urban flood exposure patterns across regions. In East Asia, especially China, UEF levels are the highest globally (Fig. 1), primarily driven by rapid expansion into flood-prone zones[10,27]. Our results show that China's UEF is projected to increase by over 50% by 2020 compared to 2015 levels, in line with earlier national studies[11]. This highlights how urban expansion in flood-prone regions directly intensifies exposure, a trend confirmed by our analysis of newly built-up urban areas (Fig. 5). In contrast, North America shows a relatively stable trend at the national level[28], but our finer-scale analysis reveals that coastal cities in the US still face considerable exposure. This indicates that subnational variation can be masked in broader-scale assessments, underscoring the value of high-resolution spatial analysis. South Asia, Southeast Asia, and Africa are experiencing a sharp rise in urban flood exposures (Supplementary Fig. S2), driven by high population densities and rapid urban expansion in flood-prone zone[29]. Future urban development in these regions must prioritize flood risk management to minimize potential losses.

Urban flood exposures are unevenly distributed between the Global South and the Global North, a pattern clearly revealed by our analysis using Gini coefficients and regional disaggregation (Fig. 6). Our results show that low- and middle-income countries, especially those in South Asia, Sub-Saharan Africa, and Southeast Asia, exhibit markedly higher levels of flood exposure relative to their urban population and built-up area. This disparity is projected to increase further under high-growth SSPs (e.g., SSP3), where rapid urban expansion continues in vulnerable flood-prone areas without corresponding improvements in flood protection infrastructure[15,17]. The socioeconomic vulnerability in these areas further amplifies the impacts of flood exposure, putting livelihoods and well-being at risk[12]. Moreover, the Gini coefficient values for urban flood exposure rise notably in future scenarios (Supplementary Table S3), indicating a growing inequality in urban flood exposure distribution across countries and regions. These findings suggest that the Global South, where both adaptive capacity and infrastructure are often limited, is likely to bear a disproportionate share of future flood risk. Strengthening international collaboration to enhance flood defense and support climate adaptation in low-income countries is therefore critical to addressing this emerging aspect of climate injustice[9]. It is also important to note that our analysis may underestimate flood exposure in some of the most vulnerable areas, as both the Global Urban Boundary[30] and projected urban expansion datasets[31] primarily capture formal urban areas. Informal settlements may be underrepresented in these datasets, particularly in low-income countries where such settlements are widespread. This data limitation underscores the need for future research to better incorporate informal urban areas into global flood exposure assessments.

Several factors play a crucial role in the formation and evolution of urban flood exposures, primarily involving flood formation, the increase in urban flood exposure, and human management strategies to mitigate exposure. Extreme climate change is a major driver of urban flooding. Global climate change has exacerbated the uneven distribution of precipitation over space and time, increasing the frequency of extreme rainfall events, including heavy storms and short-duration intense rainfall, in specific regions[32]. In cities experiencing extreme precipitation, intense rainfall over a short period exceeds the drainage system's capacity, leading to increased surface runoff and resulting in severe urban flooding[33]. Meanwhile, urbanization has markedly altered natural hydrological processes, further increasing the exposure to urban flooding. The expansion of impervious surfaces, such as roads and buildings, reduces rainwater infiltration, increases surface runoff, and leads to higher flood peaks and prolonged water accumulation[34,35]. Particularly in low-lying areas and former flood-prone zones, rapid urban expansion has replaced natural wetlands and flood detention zones, which were once essential for regulating the water cycle, increasing urban flood susceptibility[36,37]. Although climate change and urbanization drive changes in flood hazard and floodplain extents, our study relied on static 100-year floodplain data due to the current lack of globally consistent, high-resolution flood hazard projections that integrate both climate and land-use changes. This limitation, imposed by data availability and computational feasibility, may lead to underestimating future urban flood exposure, especially in rapidly developing or highly impervious regions. Addressing dynamic floodplain changes is an important direction for future research.

The high concentration of population and assets in urban areas has greatly heightened the exposure to urban flooding. The urbanization process has concentrated large numbers of residents and economic activities, further expanding the extent and impact of urban flood exposures. The high density of population and economic activities makes the potential damage and losses from urban flooding more severe[13,38]. Moreover, rapid urbanization has not only increased the occupation of flood-prone zones but also outpaced the development of urban infrastructure, making it insufficient to cope with growing demands, which further exacerbates urban flood exposures[39]. In particular, urban flood exposures have markedly increased in low-income and high-density urban areas, where limited emergency response capacity and a lack of disaster awareness exacerbate the severity of catastrophic consequences[27,40,41]. Our study's results confirm these patterns at the global scale. We found that urban flood exposure in terms of area, population, and economic value has risen sharply in rapidly urbanizing regions, particularly in low-income and densely populated areas of South Asia, Southeast Asia, and Africa. These findings highlight the unequal burden of flood risks, with vulnerable urban populations facing disproportionate exposure increases. The insufficient development of flood protection infrastructure and emergency response capacity in these regions likely amplifies their vulnerability, underscoring the urgent need for targeted adaptation strategies.

Although urban flood exposures continue to rise in some areas, effective human management actions, such as appropriate flood control measures, can substantially mitigate these exposures. The construction of dams, reservoirs, and other hydraulic infrastructure is a key strategy for mitigating urban flood exposures[2]. Many developed countries and regions possess advanced flood control infrastructure, which can reduce the impact of flooding on urban areas[12]. In recent years, flood management measures have gradually shifted towards integrated governance, which includes not only the construction of flood control facilities but also improvements to urban drainage systems[42], green infrastructure[43], and land-use planning[44]. Enhancing urban emergency management capacity and improving flood control infrastructure can effectively reduce urban flood exposures, particularly during extreme climate events, thereby mitigating catastrophic losses. Therefore, the enhancement of integrated management measures and green infrastructure is an essential part of future strategies for addressing urban flood exposures. However, due to the absence of globally consistent and publicly available data on flood protection systems, our analysis did not account for existing flood defenses. The global flood hazard dataset we adopted (from the European Commission, Joint Research Centre[45]) assumes no protective infrastructure, as it is based on topography and natural hydrological processes alone. This limitation was necessary to ensure global comparability, but it may overestimate exposure in well-protected regions. We acknowledge this as a key limitation of our study and a priority for future research, especially as more detailed global datasets become available.

This study systematically analyzed the spatiotemporal evolution of global urban flood exposures by combining historical urban area, population, and economy data for 2000–2020 with SSPs simulation data for 2030–2100, offering a comprehensive understanding of both past and future exposure dynamics. Unlike most previous studies that focused solely on one dimension, such as urban area, population, or economy, we simultaneously assessed urban flood exposures in all three dimensions (UEF, PEF, and EEF), providing multi-dimensional support for exposure analysis and expanding the theoretical framework for related research. In addition, by focusing on newly built-up areas, we revealed how urban expansion directly contributes to increased flood exposure, underscoring the close link between urban growth and flood risk. Furthermore, by applying inequality metrics such as the Gini coefficient across multiple spatial scales, including national and subnational levels as well as the divide between the Global South and Global North, we uncovered not only the overall magnitude of exposure but also its evolving inequality patterns. These findings provide scientific evidence for equitable flood risk governance, climate adaptation, and forward-looking urban planning, especially in the Global South, where the challenges are particularly acute.

This study also has several limitations. Firstly, the floodplain data used in this study were based on fixed extents of 100-year flood events and did not account for potential future changes in flood-prone areas driven by climate change, increased rainfall intensity, or urban expansion. Although some studies suggest that floodplains tend to remain relatively stable over time, particularly at large scales[10], other research has indicated that urbanization can substantially alter inundation extents. As a result, using static floodplain boundaries may underestimate future urban flood exposure, especially in rapidly developing or highly impervious regions[46,47]. Secondly, SSPs used in the study did not account for risk mitigation strategies, and their assumptions involve some uncertainty, such as land planning, infrastructure improvements, or relocation measures that managers may implement. This limits the applicability of the findings to realistic policy scenarios, which were not fully explored in the study. Thirdly, the flood hazard data did not include flood defense infrastructure due to the lack of globally consistent information, which may lead to overestimation of exposure in well-protected areas. Fourthly, both the historical and projected urban area datasets used in this study do not explicitly capture informal settlements, which may lead to an underestimation of flood exposure in these particularly vulnerable areas. It should be noted that the use of 5-year periods in the historical analysis was primarily constrained by the temporal resolution of available datasets. While this approach enables the detection of general trends in urban flood exposure, it may be affected by short-term hydrological variability, particularly in regions sensitive to ENSO cycles. ENSO typically operates on 2–5-year intervals and can markedly influence flood risk through its impact on precipitation and river discharge. As such, exposure estimates for individual 5-year periods should be interpreted with caution. Our focus remains on longer-term patterns over the full study period, and future research could incorporate ENSO indices to explicitly assess the extent of its influence on temporal variability in flood exposure. Future research should further incorporate dynamic floodplain changes, explore the interactive effects of socioeconomic development, climate change, and urban flood exposures, consider the role of flood protection measures, and improve the representation of informal urban areas by integrating socioeconomic and urban morphology datasets. Additionally, accounting for policy-related decision-making factors regarding risk mitigation and adaptation would offer a more in-depth and realistic analysis of future urban flood exposure management.

## Methods

### Defining regional divisions for urban flood exposure assessment

This study examines the characteristics of urban flood exposures at the global scale. We divide the world into 21 subcontinental regions (Supplementary Fig. S3)[2,10], and analyze the differences in urban flood exposure across various scales, including national and subnational levels[12,27]. Furthermore, to investigate the inequality of urban flood exposure in regions with different levels of economic development, we categorize the world into Global South and Global North (Supplementary Fig. S4)[48].

### Data

The data used in this study primarily consist of global river flood hazard maps, urban area data, urban population data, and urban economic data. The global 1 km resolution river flood hazard maps with a 1-in-100-year return period used in this research were developed by the European Commission[45] and have been widely utilized in flood exposure analysis[10,15,49]. It should be noted that this dataset does not account for flood defense infrastructure such as levees or floodwalls. This is primarily due to the current lack of globally consistent and detailed spatial data on such structures, including their location, elevation, and design standards. In the absence of such data, and to ensure comparability across regions, the underlying hydrodynamic model assumes natural terrain-based water flow without explicitly simulating the effects of flood defenses. While this approach supports uniform large-scale modeling, it may lead to conservative estimates of flood exposure in areas with strong protection systems. The historical urban area data are from the Global Urban Boundary dataset[30], which was developed based on the 30 m resolution Global Annual Impervious Area dataset[50], covering the period from 2000 to 2020 in 5-year intervals. Future urban expansion data are derived from global urban land expansion projections under the SSPs[50], with a spatial resolution of 1 km and covering 2030–2100 in 10-year intervals. Both datasets focus on mapping built-up urban areas with high population and economic density, and are widely used for global urban analyses. However, it is important to note that informal settlements, which are typically characterized by irregular structures and low or variable impervious surface coverage, may be underrepresented, particularly in the Global Urban Boundary dataset. This limitation could result in an underestimation of flood exposure in such areas, especially in low-income or rapidly urbanizing regions. Urban population data for 2000–2020 are from the Global Human Settlement Layer dataset[51], with a spatial resolution of 1 km, available at 5-year intervals. Future urban population data for 2030–2100 are from the 1-km grid population distribution dataset under SSPs with a spatial resolution of 1 km and updated at 10-year intervals[52]. Urban economic data are derived from the global gridded GDP dataset consistent with SSPs[53], which provides global GDP data at 5-year intervals for 2000–2020 and at 10-year intervals for 2030–2100, with a resolution of 1 km. Global administrative boundary data were obtained from GADM version 4.1. These data are publicly available and used under the terms provided by GADM. No other third-party map or image data were used in this study.

### Calculation of urban flood exposures

In this study, the flood-prone zone was defined as the maximum inundation extent based on the river flood hazard maps of 1-in-100 years return periods, which serves as a widely accepted criterion for identifying flood-prone zones. To assess urban flood exposures, this study estimated exposure by analyzing the spatial distribution of urban built-up areas, along with their population and economic data, within the flood-prone zone. The flood-prone zone was assumed static throughout the study period, following common practice in long-term exposure assessments[10,11,54]. While recognizing that some geomorphologically active areas (e.g., coastal deltas or alluvial systems) may experience boundary changes over time, maintaining constant flood-prone zones is a reasonable approach given both the uncertainties in predicting such dynamics and the need for temporal comparability in our assessment. First, flood-prone zone data are overlaid with historical urban boundaries and future urban expansion datasets to extract urban areas affected by flooding. These areas are used as indicators of UEF and serve as the foundation for subsequent population and economy exposure to flooding analyses. To better characterize the flood exposure faced by urban areas, the proportion of urban area exposed to urban flooding (PUEF) was calculated, which is the ratio of the urban area in the flood-prone zone to the total urban area of the city.

By intersecting the extracted urban flood-prone zones with the Global Human Settlement Layer dataset and future urban population growth projections, we derive the PEF. We calculate the proportion of the population affected by flooding, which is the ratio of the population living in urban flood-prone zones to the total urban population, representing the proportion of population exposure to urban flooding (PPEF).

Lastly, by combining the urban flood-prone zones with historical and projected economic data, we obtain EEF. To more accurately reflect the economic impact in urban flood-prone zones, we calculate the proportion of economic activity exposed to flooding, determined as the ratio of economic output in floodplain to the total economic output of the city, which serves as an indicator of the proportion of economic exposure to urban flooding (PEEF).

### Evaluating the inequality of urban flood exposures

Hotspot and coldspot analysis were applied to identify areas with high urban flood exposures. The Getis-Ord $G_i^*$ statistic is a commonly used method in hotspot and coldspot analysis. It detects the presence of significant clusters of high or low values by calculating the spatial relationship between a location's geographic attributes and those of its neighboring locations. The formula for Getis-Ord $G_i^*$ is as follows:

$$G_i^* = \frac{\sum_{j=1}^{n} w_{ij} x_j - \bar{X} \sum_{j=1}^{n} w_{ij}}{\sqrt{\left[\sum_{j=1}^{n} w_{ij}^2 - \frac{\left(\sum_{j=1}^{n} w_{ij}\right)^2}{n}\right] \cdot \left[\sum_{j=1}^{n} x_j^2 - \frac{\left(\sum_{j=1}^{n} x_j\right)^2}{n}\right]}} \quad (1)$$

where $G_i^*$ represents the Getis-Ord $G_i^*$ statistic value for location $i$; $x_j$ is the attribute value at location $j$; $w_{ij}$ denotes the adjacency weight between locations $i$ and $j$; $\bar{X}$ is the mean attribute value across all locations; and $n$ is the total number of spatial units. To determine whether a location is a statistically significant hotspot or coldspot, we calculated the $z$-score and corresponding $p$ value for each unit. A location is considered a statistically significant hotspot if it has a positive $z$-score and $p$ value $< 0.05$, indicating a cluster of high values. Conversely, a negative $z$-score and $p$ value $< 0.05$ identify coldspots, or clusters of low values. Values with $p$ value $\geq 0.05$ are regarded as not statistically significant and are excluded from hotspot or coldspot interpretation. This statistical framework allows for robust identification of significant spatial clusters in urban flood exposure.

The Gini coefficient was used to measure the inequality of urban flood exposures. The Gini coefficient is calculated based on the Lorenz curve, which is an important analysis coefficient used to comprehensively investigate the distribution difference. The formula for the Gini coefficient is as follows[55]:

$$\text{Gini index} = 1 - \sum_{i=1}^{n} P_i \times (2 \sum_{k=1}^{i} W_k - W_i) \quad (2)$$

where $P_i$ represents the proportion of the $i$-th region in the total area, population, or economy; $W_k$ represents the urban flood exposures of the $k$th region; $n$ is the total number of regions. The Gini coefficient ranges from 0 (absolute equality) to 1 (absolute inequality). A higher value indicates a greater inequality level of urban flood exposures, while a lower value indicates a more equal distribution of exposures.

### Reporting summary

Further information on research design is available in the Nature Portfolio Reporting Summary linked to this article.

## Data availability

The global 1 km resolution river flood hazard maps with a 1-in-100-year return period were obtained from the European Commission Joint Research Centre (https://data.jrc.ec.europa.eu/collection/id-0054). Historical urban extent data were sourced from the STARCloud platform (https://data-starcloud.pcl.ac.cn/data-nav/remote-sensing). Future urban expansion projections under the Shared Socioeconomic Pathways were obtained from the GeoSimulation database (http://www.geosimulation.cn/GlobalSSPsUrbanProduct.html). Urban population data for 2000–2020 were downloaded from the Global Human Settlement Layer (https://human-settlement.emergency.copernicus.eu/). Future urban population projections under Shared Socioeconomic Pathways were accessed via Figshare (https://doi.org/10.6084/m9.figshare.19608594.v2). Urban economic data were obtained from Zenodo (https://zenodo.org/records/5880037). Global administrative boundary data were retrieved from GADM version 4.1 (https://gadm.org/data.html).

Received: 1 April 2025; Accepted: 14 July 2025;
Published online: 28 July 2025

## References

1. Chen, X., Zhang, H., Chen, W. & Huang, G. Urbanization and climate change impacts on future flood risk in the Pearl River Delta under shared socioeconomic pathways. *Sci. Total Environ.* **762**, 143144 (2021).
2. Dottori, F., Szewczyk, W., Ciscar, J.-C. & Zhao, F. Increased human and economic losses from river flooding with anthropogenic warming. *Nat. Clim. Change* **8**, 781–786 (2022).
3. Andreadis, K. M. et al. Urbanizing the floodplain: global changes of imperviousness in flood-prone areas. *Environ. Res. Lett.* **17**, 104024 (2022).
4. Wang, Y. et al. Meta-analysis of urban non-point source pollution from road and roof runoff across China. *Earths Future* **13**, e2024EF005296 (2025).
5. McDermott, T. K. J. Global exposure to flood risk and poverty. *Nat. Commun.* **13**, 3529 (2022).
6. He, C. et al. Future global urban water scarcity and potential solutions. *Nat. Commun.* **12**, 4667 (2021).
7. Kang, J. et al. Global urbanization indirectly 'enhances' the carbon sequestration capacity of urban vegetation. *Geogr. Sustain.* **6**, 100268 (2025).
8. Jongman, B. et al. Declining vulnerability to river floods and the global benefits of adaptation. *Proc. Natl. Acad. Sci*. USA **112**, E2271–E2280 (2015).
9. Winsemius, H. C. et al. Global drivers of future river flood risk. *Nat. Clim. Change* **6**, 381–385 (2016).
10. Cao, W. et al. Increasing global urban exposure to flooding: an analysis of long-term annual dynamics. *Sci. Total Environ.* **817**, 153012 (2022).
11. Du, S., He, C., Huang, Q. & Shi, P. How did the urban land in floodplains distribute and expand in China from 1992–2015? *Environ. Res. Lett.* **13**, 034018 (2018).
12. Rentschler, J., Salhab, M. & Jafino, B. A. Flood exposure and poverty in 188 countries. *Nat. Commun.* **13**, 3527 (2022).
13. Jiang, R. et al. Substantial increase in future fluvial flood risk projected in China's major urban agglomerations. *Commun. Earth Environ.* **4**, 389 (2023).

14. Chang, H. et al. Assessment of urban flood vulnerability using the social-ecological-technological systems framework in six US cities. *Sustain. Cities Soc.* **68**, 102786 (2021).
15. Alfieri, L., Dottori, F., Salamon, P., Wu, H. & Feyen, L. Global modeling of seasonal mortality rates from river floods. *Earths Future* **8**, e2020EF001541 (2020).
16. Kam, P. M. et al. Global warming and population change both heighten future risk of human displacement due to river floods. *Environ. Res. Lett.* **16**, 044026 (2021).
17. Fox, S., Agyemang, F., Hawker, L. & Neal, J. Integrating social vulnerability into high-resolution global flood risk mapping. *Nat. Commun.* **15**, 3155 (2024).
18. Nearing, G. et al. Global prediction of extreme floods in ungauged watersheds. *Nature* **627**, 559–563 (2024).
19. Sanders, B. F. et al. Large and inequitable flood risks in Los Angeles, California. *Nat. Sustain.* **6**, 47–57 (2022).
20. Wing, O. E. J. et al. Inequitable patterns of US flood risk in the Anthropocene. *Nat. Clim. Change* **12**, 156–162 (2022).
21. Kundzewicz, Z. W. et al. Flood risk in a range of spatial perspectives—from global to local scales. *Nat. Hazards Earth Syst. Sci.* **19**, 1319–1328 (2019).
22. Hallegatte, S., Green, C., Nicholls, R. J. & Corfee-Morlot, J. Future flood losses in major coastal cities. *Nat. Clim. Change* **3**, 802–806 (2013).
23. Wu, Y. Sustainable urban planning to control flood exposure in the coastal zones of China. *Landsc. Ecol.* https://doi.org/10.1007/s10980-024-01951-8 (2024).
24. Yang, W., Zhang, J. & Krebs, P. Investigating flood exposure induced socioeconomic risk and mitigation strategy under climate change and urbanization at a city scale. *J. Clean. Prod.* **387**, 135929 (2023).
25. World Bank. *Poverty and Shared Prosperity 2020: Reversals of Fortune*. https://doi.org/10.1596/978-1-4648-1602-4 (World Bank, 2020).
26. Rogers, J. S., Maneta, M. P., Sain, S. R., Madaus, L. E. & Hacker, J. P. The role of climate and population change in global flood exposure and vulnerability. *Nat. Commun.* **16**, 1287 (2025).
27. Rentschler, J. et al. Global evidence of rapid urban growth in flood zones since 1985. *Nature* **622**, 87–92 (2023).
28. Tellman, B. et al. Satellite imaging reveals increased proportion of population exposed to floods. *Nature* **596**, 80–86 (2021).
29. Jongman, B., Ward, P. J. & Aerts, J. C. J. H. Global exposure to river and coastal flooding: Long term trends and changes. *Glob. Environ. Change* **22**, 823–835 (2012).
30. Li, X. et al. Mapping global urban boundaries from the global artificial impervious area (GAIA) data. *Environ. Res. Lett.* **15**, 094044 (2020).
31. Chen, G. et al. Global projections of future urban land expansion under shared socioeconomic pathways. *Nat. Commun.* **11**, 537 (2020).
32. Fowler, H. J. et al. Anthropogenic intensification of short-duration rainfall extremes. *Nat. Rev. Earth Environ.* **2**, 107–122 (2021).
33. Uddin, S., Revel, M., Modi, P. & Yamazaki, D. Quantifying the relative contributions of climate change and ENSO to flood occurrence in Bangladesh. *Environ. Res. Lett.* **18**, 104027 (2023).
34. Ahiablame, L. & Shakya, R. Modeling flood reduction effects of low impact development at a watershed scale. *J. Environ. Manag.* **171**, 81–91 (2016).
35. Luo, K. & Zhang, X. Increasing urban flood risk in China over recent 40 years induced by LUCC. *Landsc. Urban Plan.* **219**, 104317 (2022).
36. Bacco, M. D. Exploring the compound nature of coastal flooding by tropical cyclones: a machine learning framework. *J. Hydrol.* **645**, 132262 (2024).
37. Chakraborty, T. et al. Large disagreements in estimates of urban land across scales and their implications. *Nat. Commun.* **15**, 9165 (2024).
38. Sauer, I. J. et al. Climate signals in river flood damages emerge under sound regional disaggregation. *Nat. Commun.* **12**, 2128 (2021).
39. Nodine, T. G., Conley, G., Riihimaki, C. A., Holland, C. & Beck, N. G. Modeling the impact of future rainfall changes on the effectiveness of urban stormwater control measures. *Sci. Rep.* **14**, 4082 (2024).
40. World Bank. *Shock Waves:Managing the Impacts of Climate Change on Poverty.* https://doi.org/10.1596/978-1-4648-0673-5 (World Bank, 2017).
41. Ward, P. J. et al. A global framework for future costs and benefits of river-flood protection in urban areas. *Nat. Clim. Change* **7**, 642–646 (2017).
42. Rezaei Aderyani, R. F. & Mousavi, S. J. Machine learning-based rainfall forecasting in real-time optimal operation of urban drainage systems. *J. Hydrol.* **645**, 132118 (2024).
43. Wang, Y., Peng, L., Yang, L. E., Wang, Z. & Deng, X. Attributing effects of classified infrastructure management on mitigating urban flood risks: a case study in Beijing, China. *Sustain. Cities Soc.* **101**, 105141 (2024).
44. Huang, W., Hashimoto, S., Yoshida, T., Saito, O. & Taki, K. A nature-based approach to mitigate flood risk and improve ecosystem services in Shiga, Japan. *Ecosyst. Serv.* **50**, 101309 (2021).
45. Joint Research Centre Data Catalogue. River flood hazard maps at European and Global Scale. https://data.jrc.ec.europa.eu/collection/id-0054 (2024).
46. Gori, A., Blessing, R., Juan, A., Brody, S. & Bedient, P. Characterizing urbanization impacts on floodplain through integrated land use, hydrologic, and hydraulic modeling. *J. Hydrol.* **568**, 82–95 (2019).
47. Sun, Q. et al. Multi-scenario urban flood risk assessment by integrating future land use change models and hydrodynamic models. *Nat. Hazards Earth Syst. Sci.* **22**, 3815–3829 (2022).
48. Chen, B. et al. Contrasting inequality in human exposure to greenspace between cities of Global North and Global South. *Nat. Commun.* **13**, 4636 (2022).
49. Buttinger-Kreuzhuber, A. et al. Locally relevant high-resolution hydrodynamic modeling of river floods at the regional scale. *Water Resour. Res.* **58**, e2021WR030820 (2022).
50. Gong, P. et al. Annual maps of global artificial impervious area (GAIA) between 1985 and 2018. *Remote Sens. Environ.* **236**, 111510 (2020).
51. European Commission. Global Human Settlement Layer. https://human-settlement.emergency.copernicus.eu/download.php?ds=pop (2023).
52. Wang, X., Meng, X. & Long, Y. Projecting 1 km-grid population distributions from 2020 to 2100 globally under shared socioeconomic pathways. *Sci. Data* **9**, 563 (2022).
53. Wang, T. & Sun, F. Global gridded GDP data set consistent with the shared socioeconomic pathways. *Sci. Data* **9**, 221 (2022).
54. Güneralp, B., Güneralp, İ & Liu, Y. Changing global patterns of urban exposure to flood and drought hazards. *Glob. Environ. Change* **31**, 217–225 (2015).
55. Song, Y. et al. Observed inequality in urban greenspace exposure in China. *Environ. Int.* **156**, 106778 (2021).



## Acknowledgements
Funding for this project was provided by the National Natural Science Foundation of China (No. 42471118), the Science and Technology Program of Guangdong (NO.2023B1212070031).


## Author contributions
Qian Zhang: conceptualization, methodology, software, validation, formal analysis, writing—original draft, writing—review and editing, visualization. Chunlin Li: conceptualization, formal analysis, writing—review and editing, supervision, funding acquisition. Ding Wen: validation, supervision. Jieming Kang: formal analysis, visualization, writing—review and editing. Tan Chen: writing—review and editing. Baolei Zhang: validation, supervision. Yuanman Hu: supervision. Jiabo Yin: writing—review and editing. Louise Slater: writing—review and editing.

## Competing interests

The authors declare no competing interests.

## Additional information

**Supplementary information** The online version contains supplementary material available at https://doi.org/10.1038/s43247-025-02585-7.

**Correspondence** and requests for materials should be addressed to Chunlin Li or Ding Wen.

**Peer review information** *Communications Earth and Environment* thanks Hongyi Li and the other, anonymous, reviewer(s) for their contribution to the peer review of this work. Primary Handling Editors: Rahim Barzegar and Alireza Bahadori. A peer review file is available.